Tifft #72
Master Copy
(second version)
in 6th Reference now

DISCRETE STATES OF REDSHIFT AND GALAXY DYNAMICS II, SYSTEMS OF GALAXIES

William G. Tifft
Steward Observatory
University of Arizona
Tucson, Arizona

Received 1975 June 30
Revised 1975 December 12
Revised 1976 March 2

ABSTRACT

In the first paper in this series, a basic model was developed, for individual galaxies, consisting of two expanding opposed streams of material differing systematically in redshift. In this paper, galaxies in pairs and groups are shown to show no evidence of gravitational interaction. Redshift differentials between pairs of galaxies and between galaxies in clusters are found to take on preferred values which are various multiples of a basic 72.5 km s^{-1}. There is also direct evidence that the redshift periodicity phases together between groups to imply that there is also no large scale motion between clusters of galaxies. The various mass discrepancies or peculiarities arising from a dynamical interpretation of differential redshifts are also shown to be of a form that no gravitational interaction and no significant motion requires.

Subject Headings: Galaxies, Double Galaxies, Clusters of Galaxies, Redshift

INTRODUCTION

In the first paper of this series by Tifft (1976), henceforth called DSR I, evidence for a two redshift stream structure of individual galaxies was developed. In this paper implications of that concept are extended to pairs and clusters of galaxies. In the conventional picture, such assemblies represent successive steps in extending the concept of gravitational interaction to larger scales. The introduction of a discrete redshift has direct implications with respect to large scale gravitation. Since gravitation is viewed as the dominant large scale force inducing "observed motion," reinterpretation of the "motion" must reduce the role of large scale gravitation. It was originally considered possible that the intrinsic redshift effects might simply resolve the Virial discrepancy problem in clusters and result in normal bound groups. The apparent existence of fine structure (Tifft 1974) in the redshift distributions, however, reduces the permitted normal velocity dispersion to too small a value. This implies, assuming the observations are correct, that galaxies are relatively non-interactive gravitationally with their more distant neighbors. Thus the discussion of double galaxies and clusters in the context of the discrete redshift cannot be separated from a consideration of gravitation.

The largest scale over which conventional interaction can be considered to be "established" is the scale of a single galaxy. The theory and observations of galactic rotation are in reasonable agreement. Even for galactic rotation, as discussed in DSR I, notable deviations from a simple theory are well known. Beyond the scale of a single galaxy we have no direct evidences that normal gravitation applies.

We have, in fact, discrepancies in double galaxies and clusters which are the next steps in the scale of increasing distances. At each step the deviations become more apparent.

It is true that a good degree of success has been achieved in dynamical modeling of outlying interactive structure in a few specific double galaxies (Toomre and Toomre 1972). Considering the idealized nature of the models and the extreme freedom of adjustable parameters available the success, while certainly suggestive, cannot possibly constitute a proof. If two galaxies are close together it is obvious that local interaction in their extended material is possible just as it is within a galaxy. This in combination with the possible outflow of material from galaxies may make it possible to form outlying interactive structures without requiring that there be a net resultant force between the mass centers of the galaxies as a whole. Also, depending upon how doubles form, apparent interactions might be an aspect of formation. It is not too great a conceptual step to go from a two stream nucleus to a fissioning nucleus to produce double galaxies and a complex apparent interaction.

A much more fundamental test of dynamics addresses directly the question of continuity in what we interpret, at present, to be "velocity". If the redshift is a discrete variable, then very distinct limits can be placed upon real motion. A more basic test of large scale dynamics is difficult to imagine. The definition and application of this test is the main objective of this paper.

We will begin the analysis by considering double galaxies and investigating the differential redshift distribution in conjunction with the apparent separation distribution. If galaxies can exist only in discrete redshift states and do not have noticeable relative motions induced by interaction or any other cause, the differential redshift distribution will

be discrete at the basic periodicity, or multiples thereof, of the permitted redshift values. Even if some blurring occurs because of observational uncertainty or small real motion so that the distribution appears to be continuous, it must have the correct form if normal gravitational interaction applies. Thus both the form and continuity of the differential redshift function for pairs is a basic test of interaction and formation theories. Finally, if the discrete redshift concept is correct the form of the deviation from dynamical predictions must be consistent with discrete redshift model predictions. In order to bring the problems posed by double galaxies clearly into focus, we will first consider a purely classical viewpoint. Peculiarities arising out of this approach will then be examined as possible evidence for the multiple redshift concept.

THE CLASSICAL VIEWPOINT

A double galaxy is effectively described by specifying the apparent separation, the redshift difference between the components, and the combined or individual magnitudes. The luminosity is related to mass through the M/L value. In the conventional picture, the separation and differential redshift are related to the actual separation and relative velocity by projection factors. Any double system is described by two vectors, one specifying position, the other velocity of one galaxy with respect to the other. These two vectors, r_o and ΔV_o, regardless of orbital models, can be presumed to be isotropically distributed outside of local inhomogeneities. If θ and ϕ are the angles between the line of sight and the vector direction, for r_o and ΔV_o respectively, then the observed separation and differential velocity are given by:

$$r = r_o \sin\theta \quad , \quad \Delta V = \Delta V_o \cos\phi . \qquad (1)$$

If N_o pairs are considered the distribution of numbers with θ or ϕ is given by:

$$\frac{dN}{d\theta} = 2\pi N_o \sin\theta \quad , \quad \frac{dN}{d\phi} = 2\pi N_o \sin\phi . \qquad (2)$$

For each particular value of r_o and ΔV_o the cumulative distribution of r and ΔV are given by:

$$\frac{dN}{d\Delta V} = \frac{dN}{d\phi} / \frac{d\Delta V}{d\phi} = \frac{2\pi N_o}{\Delta V_o} \quad , \quad \frac{dN}{dr} = \frac{dN}{d\theta} / \frac{dr}{d\theta} = \frac{2\pi N_o}{r_o} \tan\theta \qquad (3)$$

Thus for any r_o, and ΔV_o values, the apparent distribution of ΔV is flat between zero and ΔV_o while r is sharply peaked toward r_o. Figure 1 illustrates the distributions.

The observed distribution of r and ΔV for all possible values of r_o and ΔV_o will be superimposition of these specific functions weighted according to the frequency of particular r_o or ΔV_o values modified by any selection effects in the sample. The observed ΔV_o distribution can, for example, be thought of as a largest ΔV_o rectangle upon which are stacked successively smaller rectangles. The observed ΔV_o distribution must therefore show a monatonic rise toward zero. The distribution of separations is such that half of all pairs will be seen within 13% of their actual separation. Selection effects may modify these conclusions slightly, but corrections will depend upon the type of orbital motion assumed. The usual selection effect considered is a tendency to omit a disproportionate number of the widest pairs. It is intuitively obvious, and formally shown by Noerdlinger (1975) that if orbits are circular, this omission will lead to a deficiency of high ΔV pairs. On the other hand, if orbits are highly elliptical, a deficiency in low ΔV pairs will result. Without knowing in advance what orbital pattern or distribution is actually present, the correction is indeterminate. Hopefully other information may give some

insight to the problem which will be considered further in later paragraphs.

For any gravitationally bound pair the relative velocity must rise for increasing mass or decreasing separation, all other conditions remaining equivalent. The specific function for circular orbits is:

$$\Delta V_o \propto M^{\frac{1}{2}} R^{-\frac{1}{2}} \qquad (4)$$

where M is the sum of the individual masses. Because of evidence to the effect that M/L ratios depend upon morphology, galaxies should be treated in subgroups, according to whether they are spiral-spiral, spiral-elliptical, or elliptical-elliptical pairs.

The best available current summary of redshifts for double galaxies appears to be from Karachentsev (1974). He presents collected data for 101 isolated pairs giving classifications, separations, the redshift differences and a measure of the accuracy of each difference. The data were utilized by him to derive M/L values for various classes of galaxies. Except for the most interactive types, he found M/L to be essentially independent of type and about five times larger than the values derived from individual galaxies. He therefore concluded that the usual mass discrepancy problem is present. In a general discussion of dynamical systems including double galaxies, Rood (1974 with previous references) finds the same mass discrepancy and further shows that the mass discrepancy increases directly with $(\Delta V)^2$.

The typical total magnitude of the systems studied by Karachentsev (1974) is Mp = -21.0 with 75% falling between -20.0 and -22.0 (H = 75 was used by Karachentsev). The average apparent projected separation is close to 20 kpc. The typical Karachentsev double is therefore as or more luminous than the Galaxy or M31. For normal M/L values the typical Karachentsev spirals will have masses greater than or comparable to the Galaxy, and in the case of ellipticals perhaps have significantly greater mass. Therefore, typical Karachentsev doubles would be expected to have relative velocities

similar to and in many cases greater than the solar circular velocity in the Galaxy.

In Figure 2 the relationship between ΔV and the combined magnitude for the Karachentsev (1974) double galaxies is shown. The pairs are separated according to spiral-elliptical morphology. Two features stand out in Figure 2:

1) There is a distince trend away from small ΔV as one goes from spirals to ellipticals.

2) There is a large concentration of luminous spirals with low ΔV.

The first point can be interpreted conventionally to mean that ellipticals have higher masses than spirals, hence larger ΔV. We will return to a discussion of the ellipticals later. The second point is more difficult to explain. It cannot be due to velocity projection effects since it was previously shown that the distribution of ΔV is flat for any given ΔV_o. Selection effects offer little remedy either. First, one must assume circular orbits to select against high ΔV at large separations. It was previously shown that the majority of doubles will be seen at nearly their true separation. For every point of very low ΔV that one wishes to account for by selection one must overlook a sizeable number of wide pairs. There clearly is a limit before one is "omitting" far too many physical pairs. This is obviously inconsistent with studies of the frequency of galaxy pairing as a function of separation as compared against expected accidental pairing. Further, even if one insisted on pushing the selection to extremes assuming circular orbit spiral pairs one would then have to explain why the elliptical pairs escape such selection. Since the selection cannot obviously differ, the orbital character must be radically different, a point of view which is not readily justified. Finally, the insistence

on circular orbits cannot be substantiated as further discussed below. One is finally led to conclude that a conventional interpretation of the strong peaking of ΔV at low values appears to require that many galaxies have low ΔV_o. This point seems to have been ignored previously in the literature. Figure 3 gives the ΔV distribution function for spiral-spiral pairs with combined Mp < -19.0 and for two other classes of galaxies to be discussed later.

Low ΔV_o can arise in conventional dynamics either by having large separations or small total mass. The lower left panel of Figure 4 gives the distribution of the projected separations for the spiral-spiral pairs with combined Mp brighter than -19.0; the distribution rises toward zero. Since the distribution function of projected spearations was previously shown to peak sharply near the real separation, the only way to produce the observed distribution is to have many small real separations. As mentioned above, there is a distinct limit to the enhancement of small separations permitted by selection before an obvious excess of wider pairs appears. It is therefore clear that the small ΔV galaxies cannot arise from a large population of wide pairs. A real concentration of very luminous galaxies with low mass is implied. This is a very curious result considering that M/L for spiral-spiral double galaxies on the average is quite large.

The upper left panel of Figure 4 shows that there is no dependence of ΔV on separation. This effect has been previously noted by Zonn (1968) and Rood (1974 with previous references). The most luminous pairs, those with Mp < -21.0 are shown with larger symbols to illustrate, along with Figure 2, that the most luminous pairs have the smallest range of ΔV. This means that the most luminous galaxies have the largest percentage of the smallest real relative velocities. The lack of dependence of ΔV on separation has been used by Zonn (1968) to argue that many double galaxies are in radial

unbound or hyperbolic motion. It clearly argues against the circular orbit model discussed earlier. If this interpretation is correct, then Figure 3 illustrates that in many spiral-spiral pairs, many with luminosity in excess of the Galaxy, the hyperbolic velocity at 20 kpc separation is less than 200 km s^{-1}. If true, we again conclude that very low mass is involved. The flatness of the ΔV-separation diagram could be used to argue for mass distributed at larger radii (massive halos) which prevent the drop in ΔV with increasing separation. In order to be invisible such large amounts of mass would have to have large M/L. However, M/L for the entire system is known to be low, hence no dominant mass of high M/L is permitted.

The most extensive discussions of the dynamics of double galaxies utilize the distribution of calculated masses and the distribution of calculated scale factors between true mass and mass derived from ΔV and separations. Karachentsev and Shcherbanovsky (1970) considered several different orbital models and concluded that either unbound systems or circular orbits could fit the distribution of calculated masses. They did not, however, distinguish galaxies morphologically and did not address the problem of the large number of low ΔV galaxies at low separations. It is a sizeable number of intrinsically low velocity galaxies that produce the spike in the observed mass function near zero, not simply projection or selection factors. The mass distribution loses much of the information contained in the ΔV distribution since ΔV enters the mass calculation as the square. Despite the lowered sensitivity of the observed mass distribution, Page (1952) using a circular orbit model was able to show that to fit the distribution two distinct masses of galaxies were required. A very low mass was required to fit the central spike and a much larger value was required to provide the high masses present. Intermediate masses or a

continuous spread of mass would not fit the distribution. The distribution is high at both ends and low in the middle. Such an effect appears consistently in double galaxy studies. See, for example, Jenner (1974) with reference to supergiant ellipticals. Figure 5 is a plot of M/L as a function of Mp for the Karachentsev spiral-spiral pairs. The strong clumping at M/L<1 is obvious as is the scattering of large M/L values. One further point is shown by the line labeled "constant M". The low luminosity galaxies which show respectable M/L values have the same masses as the very luminous galaxies of low M/L. The difference arises solely from the different luminosities.

To summarize the spiral-spiral double galaxy problem, it appears necessary to distinguish a very low mass class of luminous spiral galaxies. This class is apparently not continuous with more massive types. The usual method of averaging M/L over numerous pairs produces an average which represents neither the "high" nor "low" mass spirals.

Consider now double galaxy pairs containing ellipticals. As previously mentioned, such pairs tend to show fewer low ΔV values than spiral-spiral systems. The center panel of Figure 3 shows the distribution function of ΔV. Two interpretations of the distribution appear possible; it may be rectangular with a maximum ΔV_o near 350 km s^{-1} or it may show a slight central peak and a secondary peak near 280 km s^{-1}. The number of points is too small to distinguish between the two suggestions. For an unbiased sample in the dynamical model the distribution of ΔV must be flat or rise monatonically toward zero; a real secondary peak should not exist. The lack of a rise toward zero implies that only a narrow range of ΔV_o is present in such pairs. Six scattered points between 400 and 700 km s^{-1} are off scale in the figure but too few in number to markedly change the conclusion.

In most investigations such high ΔV galaxies cannot be distinguished from optical pairs and may not represent real doubles at all.

Evidence supporting the reality of a second peak in the ΔV distribution is given in the lower panel of Figure 3. This panel shows the ΔV distribution for double galaxies which Karachentsev (1974) classifies as showing no signs of interaction. The distribution is apparently double although the numbers are small. Two thirds of the points in the outer peak arise from pairs containing ellipticals, hence the peak is tentatively associated with ellipticals rather than spirals. The outer peak has a mean ΔV of 285 km s^{-1} and the six points show an rms scatter of only 18 km s^{-1}. This secondary peak has been previously noted by Gorbachëv (1971). His galaxy sample is not specified and presumably includes many or all of the Karachentsev objects. The galaxies were apparently independently classified, and the peak in Gorbachëv's study includes more than a dozen pairs, hence there is some element of independence. Gorbachëv suggests that the galaxies could represent optical pairs. Karachentsev (1974) concluded, however, that no more than one optical pair with $\Delta V<300$ km s^{-1} was likely in his sample. Only three optical pairs with $\Delta V<1000$ km s^{-1} were considered likely. Furthermore, the number rises smoothly with ΔV and should not show a well defined peak. We therefore conclude that there is evidence for a secondary peak in the ΔV distribution of pairs containing ellipticals.

Some additional information on ellipticals is contained in the distribution of separations. The lower right side of Figure 4 indicates that the elliptical pairs occur preferentially at separations of 10 to 25 kpc with a distinct drop at wider spacings and no peaking at small separations. From the expected distribution of separations, the implication is that the majority of the pairs have real separations near 20 kpc. The ΔV-separation diagram for ellipticals in Figure 4 indicates no obvious trend of ΔV with separation.

The group of objects responsible for the 285 km s^{-1} peak can be seen.

In summary, three points emerge from the double galaxy analysis which bear on the redshift question:

1) The average dynamical M/L over all pairs shows the usual "mass deficiency" and the mass deficiency increases directly with $(\Delta V)^2$.

2) Spiral pairs appear to require a dual mass model to account for the large number of low ΔV_o values.

3) Elliptical pairs, especially in systems without direct interactive symptoms, appear to show a secondary peak in the ΔV distribution at ΔV=285 km s^{-1}.

THE DISCRETE REDSHIFT

In the previous section the peak of ΔV near zero was discussed. It was shown that if gravitational dynamics applies, a major portion of double galaxies can be inferred to have low intrinsic mass. Figure 6 gives the ΔV distribution for the complete Karachentsev (1974) sample up to 600 km s^{-1} and for the best subsample, those listed with uncertainties $\leq$100 km s^{-1}. For the full sample 43% have ΔV<90 km s^{-1} and 25% have ΔV<50 km s^{-1}. The average uncertainty in ΔV quoted by Karachentsev is 108 for the entire sample and 66 for the best sample. It is clear, therefore, that the sharp peak "near" zero cannot be distinguished from one which is identically "at" zero and smeared purely by observational uncertainty. There are larger ΔV values which are certainly not equal to zero, however a <u>series</u> of peaks at zero and multiples of 70-75 km s^{-1} can clearly represent the distribution. Such a pattern will specifically account for the 285 km s^{-1} peak and the low ΔV peak which produces the low mass peculiarity. If ΔV has nothing to do with

motion then mass calculated using $(\Delta V)^2$ will show a $(\Delta V)^2$ dependency compared with "visible" mass. Thus all the observations which are dynamically "peculiar" are predictable consequences of the multiple redshift concept providing that we also assume that there is no significant real motion which would blur the pattern. Thus coupled with the multiple redshift concept we have direct evidence for the idea that the mass centers of individual galaxies do not gravitationally interact.

Two critical tests of the multiple redshift-non interactive galaxy idea vs. gravitational dynamics are implied in the above paragraph. If the new concept is correct the peak "at" zero should sharpen when improved data becomes available until implied dynamical masses become untenably small. Secondly, the existence of real peaks in the ΔV distribution away from zero is not permitted by the projected distribution of dynamical velocities. Neither of these tests are definitively possible at this time, however, the manifestations were clearly seen in the dynamical discussion. In order to demonstrate the periodicity test a power spectrum of the best sample of Karachentsev data in Figure 6 was calculated. Figure 7 contains the power spectrum. The best sample was used since to detect a periodicity P the rms uncertainty in the data must be less than about P/3, preferably less than P/4. Even the best available data on double galaxies are therefore insufficient to detect effects at 100 km s^{-1} resolution. This limitation in general explains why many of the effects discussed in this series of papers, if real, were previously detectable only indirectly.

The power spectrum in Figure 7 shows a peak of 7.4 at 128 km s^{-1}. Even without advance prediction such a peak has only a 3% chance of accidental occurrence. Small power modulations occur near 210 and 280 but lie on the wing of the periodicity set by the full range of values and are difficult to interpret. At first sight the observed peak periodicity appears somewhat

low for a multiple of 70. This is, however, a direct consequence of uncertainty in ΔV. Values close to zero will systematically be moved away from zero by errors in measurement, hence the effective position of the zero peak taken without regard to sign is always displaced toward the higher peaks and reduces the period observed. Thus the true dominant period must be slightly longer than 128 and is therefore consistent with 140. In general overview of the double galaxy data, it is difficult to escape the conclusion that the multiple redshift and non-interactive galaxy concepts are more consistent than conventional gravitational dynamics.

The resolution of the available ΔV data prevents one from seeing if a peak in ΔV near 70 is present in double galaxies. It is possible to say, however, that ΔV near zero and 140 are found primarily in spirals while higher ΔV, especially near 280, favor ellipticals. A further feature of interest in double galaxies concerns the rate of separation if, as suggested above, the components are totally unbound. In order to detect the redshift state spacing, the galaxies can have random relative real motion no larger than a few tens of km s^{-1}. At a speed of 10 km s^{-1} it requires 10^8 years to move 1 kpc. Thus unless separation speed was much higher at some earlier time a double object will persist for a long time.

DOUBLE GALAXIES AS ACTIVE OBJECTS

The idea that double galaxies might form from fissioning and that many pairs might be unbound is not new, although the concepts and reasoning behind the idea of large scale non-interaction of galaxies is new. With gravitational binding, the mechanism and energetics of fissioning or ejection have been vague beyond recognition that early stages would involve "active" objects. In the present multiple redshift concept, the activity may consist of the

development of a pattern of redshift states in the original nucleus which is incompatible with maintaining a stable two stream flow pattern. As in the case of any major transition a period with a high level of optical activity seems likely. Heidmann and Kalloghlian (1973, 1975), Casini et al (1974) and Casini and Heidmann (1975) have discussed the occurrence of Markarian and compact galaxies in pairs and concluded that pairs contain an excess of such active galaxies. A production scheme which involves the ejection of compact objects from a parent body with subsequent decay toward normal galaxies has been proposed by Casini et al (1974). Ambartsumian (quoted in Heidmann and Kalloghlian 1975) prefers a direct fragmentation or fissioning of the parent body rather than ejection.

In order to clarify some of the critical questions relating to double galaxies a program of redshift spectroscopy of the Karachentsev (1972) double galaxy catalog was undertaken by the author at the Steward Observatory. Spectrograms now exist for all 324 Karachentsev doubles with separations $\leq$80" and a few of the 279 with separations >80". Optical activity is clearly the rule rather than the exception in this statistically complete sample of objects. Within the sample of 324 pairs with separations $\leq$80", 51% of the pairs contain two emission line galaxies and an additional 20% of the pairs have one emission line object. Overall 64% of the more than 600 individual galaxies involved show some degree of emission line activity and in more than 25% the activity is strong. Detailed analysis of the data is now beginning.

The galaxies with the strongest emission lines have been selected for high dispersion spectroscopy since preliminary analysis has suggested some peculiarities in redshift and emission line structure. A number of cases of emission line doubling especially in the forbidden lines have been observed.

In general, the emission lines are not broad; 3727 is normally easily resolved but the lines are often structured. In all cases so far observed line splitting occurs in multiples of 70-75 km s^{-1}. Plate 1 illustrates the best cases presently observed and descriptions of each object shown are given here.

K 104=IC 396ab. Karachentsev describes this object as a double of 12" separation, class LIN(ta), but indicates in notes that it may be a single galaxy. Both visually and spectroscopically, it appears single with some diffuse emission away from the nucleus. Although it certainly is single, it is included here becasue it well illustrates the dual redshift pattern and nuclear redshift discontinuity in single galaxies. Plate 1a is a 47A mm^{-1} spectrogram at Hβ taken in position angle 96^{o}. Sharp slightly tilted Hβ features appear on either side of the nucleus and give no indication of continuity. Projecting the tilted lines to the nucleus gives ΔV_o=83.

K 466=Arp 90=NGC 5929/30. This beautiful pair of spiral galaxies has a separation of 29" in position angle 48^{o} and is classified LIN(br) by Karachentsev. Published redshifts of 2868 and 2683 gives a ΔV_o=183 which is not consistent with the dual redshift hypothesis. Inspection of Plate 1b shows, however, that emission is present in both nuclei and is double for all lines in the brighter galaxy. The single weaker emission line in the fainter galaxy is rather broad. The two components of emission in the brighter galaxy are slightly spatially displaced laterally and differ in redshift by 288 km s^{-1}. The redshift difference between the <u>mean</u> of the doubled lines and the mean position of the broad line in the fainter galaxy is 180 in close agreement with the published values. It is obvious, however, that the redshift differential in the system is <u>not</u> 180. The broad line in the fainter galaxy is consistent with two redshifts spaced by 70-75 so that

four redshifts are suggested. Two turn out to be essentially identical and the other two are spaced by 288 and 70-75.

K 144. This object has a separation of 32" in position angle 143° and is classified as non-interactive by Karachentsev. Morphology of the pair is E-SO. Spectroscopically the pair is somewhat similar to K 466 excepting that [OIII] is much weaker and Hβ is sharp in the second component. The line doubling is very similar. Giving the weak [OIII] half weight, the line splitting is 297 km s^{-1} and is one of the more uncertain determinations. The mean redshift of the double lines is close to the redshift of the companion, however, the internal scatter between Hβ and [OIII] is too large for a good comparison and a deeper spectrogram is required. The emission is weak enough in this galaxy that H and K absorption shows clearly in a low dispersion spectrogram of the system. H and K are narrow in the single line galaxy and broad in the double line galaxy suggesting that the same duplicity of states is present in the stellar absorption component.

K 363=NGC 4922B=5C4.130. This galaxy is the fainter component of a double galaxy in the northern part of the Coma cluster. Karachentsev classifies the pair as ATM(am). The primary, NGC 4822A, is a normal absorption line elliptical galaxy 22" distant in position angle 210°. Low dispersion spectra of the galaxies have been described by Tifft and Tarenghi (1975). The best redshift data are summarized by Tifft and Gregory (1976). The line splitting in this galaxy occurs only in [OIII] and the components are unequal and rather broad, as is Hβ. The line splitting in N2 is 365 km s^{-1} and somewhat less but poorly determined from N1. The mean redshift of Hβ is nearly identical to the mean of [OIII]. At low dispersion [OIII] appears higher because of the unequal strengths of the unresolved components. This is the largest splitting so far observed, and closely equals five states. All of the components are sufficiently broad that they could easily be blends of two

adjacent states or be widened by appreciable real internal motions. This galaxy, therefore, closely resembles the type II Seyfert class of objects. The redshift difference between K 363A and B according to Tifft and Gregory (1976) is 222 km s^{-1}.

K 288=VV 118=Arp 299=Mark 171ab=NGC 3690+IC 694. This pair of complex spiral galaxies is classified DIS(2) by Karachentsev and has a separation between centers of 23" in position angle 88°. The position angle is somewhat uncertain because of the complex lumpy nature of the galaxies. Several redshifts have been published; the ones most comparable to this study are by deVaucouleurs and deVaucouleurs (1967) with a slit in position angle 80°. Their values were 3097 and 3212. Apparently no previous study utilized a dispersion sufficient to detect the great complexities in line structure shown in Plate 1e. The component with the weakest continuum is obviously doubled in redshift and spatially. The second component is also apparently double but the great strength of the stronger component limits the visibility of the second feature to a weak tail at longer wavelengths on the inside of the system. In addition to the splitting a general tilt, presumably due to rotation, slightly inclines the lines. The lateral offset of the doubling requires that a correction for the rotation be applied; 15 km sec^{-1} corrections have therefore been made to each component to refer to the mean of each galaxy. The offsets are small enough that the exact value of the tilt is not critical. After this correction the differential redshifts for the obvious double is 207 km sec^{-1} and for the other pair 65 km sec^{-1}. The latter is somewhat uncertain. The mean redshifts of the two pairs agree within 6 km sec^{-1} and the four values form a set with intervals 65-65-77 for a mean of 69.

K 181=Arp 202=NGC 2719ab. This pair has a separation of 32" in position angle 172°. Karachentsev classifies the pair as DIS(1) and notes that the southern component might itself be a double. Published redshifts are 3073 and 3210. This object is interesting in that the doubling, which by now will be seen to be a persistent property of the galaxies illustrated,

is almost entirely spatial. The small net difference of 15 km sec^{-1} between the two close knots presumably indicates rotation. The redshift difference between the mean of the bright knots and the second galaxy is 85.

K 252=IC 649ab. This most extraordinary object is classified ATM(sh) by Karachentsev. It has a separation of 14" in position angle 172^{o}. Morphologically, on image tube direct photographs, the object looks somewhat like a pair of opposed commas, the southern being the brighter. Both long and short wavelength spectrograms are reproduced in Plate 1. The comma shaped morphology leads one to expect some component of rotation between the laterally separated knots in the spectra. Some tilting and enlongation, especially visible in the 3727 components, is present in the direction generally joining the northern and southern pairs of knots. There is no indication of any rotational tilt joining the two strong knots. The correction due to rotation between the strong knots appears not to exceed 10 km sec^{-1} and is sufficiently uncertain that it has been ignored. The mean redshift separation of the two strong southern knots is 277 km sec^{-1} based upon N2, Hα, Hβ, and H8 which show excellent internal agreement. [NII] and 3727 give comparable but much less reliable values. The most surprising thing is that [NeIII] 3868 gives a well determined Δv_o=62 km sec^{-1}! The low [NeIII] value is confirmed from Hε+[NeIII] which gives a value of 149, between the individual expected values. The absolute redshift of [NeIII] is in agreement with the other lines in the southernmost knot. It differs radically in what would be considered the nucleus of the southern galaxy in the pair. The [NeIII] differences are easily seen in Plate 1. The only features in the northern galaxy which could be usefully measured were 3727 and Hα. The 3727 measures indicate a difference between the two

northern components of only 12 km sec^{-1} while Hα indicates a slightly larger value. The overall mean redshift, from 3727, of the northern knots differs from the southernmost knot by 149 km sec^{-1}.

K 83=VV 331=Arp 118=NGC 1143/44. This object is another most unusual system which apparently has no previous spectroscopy. The pair is separated 43" in position angle 119°. Karachentsev classifies it as ATM(sh). Photographs of the object show shreds of material scattered about in the system. Both galaxies show absorption and the western galaxy shows some possible weak 3727. The eastern galaxy shows moderately strong emission which is clearly doubled. The lines also appear somewhat broadened and only N2 can be accurately measureed; it gives ΔV_o=294 km sec^{-1}. The most remarkable features of the system are most easily seen from 3727. A patch of material to the outside of the system has a higher redshift, and will be called patch H. A patch of material between the two galaxies has a lower redshift and will be called patch L. Both patches H and L appear to connect to the easternmost galaxy be very fine lanes of emission. A lower dispersion plate shows the features clearly in [OIII] and [NII] as well as at 3727. The total redshift range H-L in 3727 is 1012 km sec^{-1}. Since the main doubling is not separable in 3727 and the outlying features are very weak at N2 the redshift differentials between H and L and the main knots are uncertain. The absolute redshifts show small systematic effects with wavelength so that only differentials have maximum reliability. N2 alone gives a differential L to the lower redshift component of the doubled emission of 274 km sec^{-1}. Matching the mean of 3727 with N2 gives a differential of 255. Neither value should be considered reliable.

The previous sample of objects provides a useful insight into several important aspects of double galaxies. The eight objects discussed represent

one fourth of the systems so far examined at 47A mm^{-1} dispersion, and does not represent all the unusual objects in the sample. It is apparent, therefore, that perhaps 25% or more of doubles with strong emission will show redshift peculiarities. The differential redshifts at 47A mm^{-1} on well defined features are not likely to be in error by more than 20 km sec^{-1}. The sample discussed generally supports the small redshift differences found in pairs and noted earlier. The objects considered have been close pairs where expected orbital velocities should be high. When well defined line doubling has been seen, it is consistent with multiples of 70-75 km sec^{-1} redshift state spacing. When differentials between galaxies can be derived the same characteristic redshift intervals are apparently involved although accuracy is less in such comparisons. The common occurrance of line splitting near 285 km sec^{-1}, identical with the suggested secondary peak in Δv between galaxies in pairs, should be noted. Table I summarizes the line splitting differentials.

When multiple redshifts appear it is quite unclear what differential redshift should be used from the dynamical viewpoint. Several cases of blended multiple emission lines, like K 466, must exist in the literature and in general the accuracy of many existing redshifts is low. Most of the emission splitting observed has been seen on the strong emission line objects in the closer pairs. At the moment selection plays an important role in the statistics. Some data are available but complete sample statistics have not yet been compiled on the dependence of emission activity or line complexity on each other or on galaxy separation or morphology. Thus, the preliminary results should be interpreted with caution. It is equally uncertain what fraction of single galaxies with emission will show peculiarities.

In addition to the redshift splitting a two region spatial splitting of the emission regions in the active objects was also generally noted. Such a separation bears a direct resemblance to the two stream situation in normal galaxies excepting that a higher multiple of the redshift state spacing is involved. Double galaxies obviously have a key role to play in understanding the redshift and the basic nature of large scale forces between galaxies. If conventional dynamics is the answer then there are some major discrepancies in need of explanation.

CLUSTERS OF GALAXIES

In the previous sections of this paper an attempt was made to use double galaxies to evaluate the nature of large scale forces between galaxies. The conclusion drawn is that no significant net force can be demonstrated to exist between separated galaxies. The next extension and test of this idea invokes clusters of galaxies. For a cluster all objects are at the same distance hence effects arising on the intercluster scale can be avoided. Since a cluster occupies a limited part of the sky, uncertainty in galactic rotation corrections are also minimized. If no net force or resultant motion exists between galaxies, the cluster members should show only specific discrete redshifts spaced by the basic interval of 70-75 km s^{-1} or its higher multiples.

Difficulties arise immediately if one attempts to apply a 70-75 km s^{-1} periodicity test directly. In order to detect a periodicity of 70-75 km s^{-1}, individual redshifts must have accuracies approaching 1/4 of the periodicity, or about 20 km s^{-1}. Little information of this caliber has previously existed for any cluster. Typical low dispersion redshifts available are good to about 100 km s^{-1}. For double galaxies the situation is sometimes slightly

better since differential redshifts may often be derived from a single spectrogram. Rotation measurements within a single galaxy are also often differential, hence more reliable. A second problem arises from the fact that overall mean redshift in a galaxy on the two stream hypothesis is automatically a blend of two or more states so that each galaxy must be investigated in detail to unravel the specific states involved. This problem was well illustrated in the previous discussion of emission line double galaxies. A third point to be kept in mind when examining clusters is that many of the strongest bits of evidence for a discrete redshift have come from emission line galaxies. Important exceptions, in M31 in particular, imply that absorption lines show the same effects, but the case is not as certain. Most galaxies in major clusters show only absorption lines.

Through one fortuitous circumstance, however, it appears that one form of the redshift periodicity can be fairly easily detected in clusters. That circumstance is that not all states appear equally likely to occur, thus in an assembly of many objects a higher order modulation of the state population can appear. This effect, which was already implied to some extent in double galaxies, is perhaps best introduced via the Local Group where individual state spacing can apparently be seen. Figure 8 gives the redshift distribution in the Local Group using redshifts from deVaucouleurs and deVaucouleurs (1964). No attempt has been made to improve any redshifts based upon the specific states now suggested for any of the local galaxies. Thus the same opportunity for state blending occurs in all objects and the data are uniformly selected. Four states are represented with the usual spacing near 70-75 km s^{-1}. One important point apparent in Figure 8 is that most galaxies clump at one redshift within the wider interval of states.

It was previously shown by Tifft (1974), based upon a preliminary

analysis of the best redshifts in the Coma cluster, that a redshift periodicity of 222 appeared to be present. The significance of 222 as three times the proposed basic state spacing was not apparent at the time but is now seen as a possible modulation of state population as perhaps seen in the Local Group. Note that even the detection of a periodicity of 200 km s^{-1} requires redshift accuracy on the order of 50 km s^{-1}, thus any such periodicity is not likely to have been seen previously. Before presenting the newest test for the 222 km s^{-1} periodicity and individual 70-75 km s^{-1} state spacing we shall first consider the current condition of redshift data for the Coma cluster.

Table 2 contains redshift information on 78 galaxies, within 6^{o} of the center of the Coma cluster, which have the most reliable redshifts. The data are extracted on the basis of redshift accuracy alone from a complete sample of Coma cluster galaxies (Tifft and Gregory, 1976). The redshift interval 6500-8000 is separated for reasons given later and the galaxies are grouped by redshift accuracy criteria. The first column gives the Zwicky identification number, which consists of the field number from Zwicky and Herzog (1963), followed by a running serial number for the list of galaxies in each field. Note that 160A refers to the special list of galaxies in the center of the Coma cluster. The second column gives other identifications. N and I refer to NGC and IC numbers, while RB refers to Rood and Baum (1967), TT to Tifft and Tarenghi (1975) and C6.124 is one of the newer Westerbork radio sources. The third column gives the redshift corrected for earth orbital motion and galactic rotation (300 km s^{-1}). The letter "E" attached to a redshift means emission is present. The fourth column gives the redshift source, and the last two columns give the photographic magnitude from Zwicky and Herzog (1963) and the distance in degrees from the cluster center.

The subdivisions in the data include one where central Coma galaxies have been observed from 3 to 5 times, hence providing a more accurate mean redshift. These values are denoted C3, C4, or C5 in Table 2. The details of source notation have been described by Tifft and Gregory (1976). Twenty-two of the twenty-five redshifts in this class have unpublished redshifts by Gunn and Sargent (personal communication) at higher dispersion. Omitting one with a very large residual, comparison of these two sets of redshift gives a mean difference Tifft - Gunn Sargent of +20±15 (mean error of mean) and an rms scatter σ_{T-GS}=68. These comparisons are pessimistic in that they include earth orbital corrections for the Gunn and Sargent values unavailable to the author. Ignoring the corrections and assuming that errors distribute uniformly between the two sources, the typical C3 redshift would have $\sigma \simeq 48$ km s^{-1}. Internal comparisons of the multiple values give an uncertainty closer to 30.

The second subdivision compiles the strongest emission line galaxies since emission line galaxies generally yield more accurate redshifts. Approximately 100 emission line galaxies are now known within 6^{o} of the Coma center and a nearly complete set of spectrograms exists. Many of the galaxies show only weak 3727, however a number show strong lines of hydrogen and [OIII]. Table 2 contains information on 35 galaxies with relatively strong emission and an available redshift. Most of the Steward Observatory (C, E and H sources) redshifts are from Tifft and Gregory (1976). For strong emission line galaxies which have not yet been measured by the author on Steward spectrograms, other published redshifts have been used temporarily. All these values are from the summary by Tifft and Gregory (1976). Too few intercomparisons between sources are presently available to evaluate the emission line redshift accuracies, however, there appears to be no reason to doubt the quality of these values.

The third redshift quality group utilizes the total collection of spectrograms of absorption line galaxies out to a 6^{o} radius centered on the Coma cluster. Many of these spectra are of excellent quality. The galaxies have been grouped according to the redshift residual between the H and K lines. Eighteen galaxies with CaII K-H redshift differentials <50 km s^{-1} are included in Table 2.

Figure 9 presents the redshift-magnitude diagram of the 43 galaxies in Table 2 with 6500<Vo<8000. It also gives the redshift projection and power spectrum of the redshift distribution. The power spectrum peak of 10 at 225 km s^{-1} leaves little doubt that a periodicity of three times the basic state spacing exists in the 6500-8000 km s^{-1} interval of the Coma cluster. The original identification of the periodicity (Tifft 1974) utilized only 31 data points. The 40 percent increase in sample reported here fully confirms the previous result. The well determined absorption line redshifts are important contributors to the periodicity and should contribute to removing doubt that both emission and absorption - both gas and the stellar substratum - participate in the discrete nature of the redshift. Note that the presence of a demonstratable and repeatable fine structure pattern in the redshift distribution in a cluster in itself places stringent limits on the gravitational interaction and resultant motion possible between galaxies. After allowing for redshift uncertainty any possible remaining internal Doppler effect in the Coma cluster cannot exceed a few tens of km s^{-1} or the pattern could not be seen. The visible mass alone on a conventional Virial Theorem analysis requires much more motion than allowed. Thus, even ignoring the fact that the fine structure falls at a predicted periodicity, the simple existence of the fine structure requires that galaxies be by and large non-interactive.

Up to this point nothing has been said about redshift-magnitude bands. The redshift interval indicated in Figure 9 represents a single band, the prominent brightest band in Coma. The lower redshift galaxies fall on other bands and the highest redshift objects may include fragments of higher bands. It appears that some of the objection to the significance of the author's previous work on redshift-magnitude banding arose from a concern that magnitude is an ill defined and relatively inaccurate quantity for a galaxy. This paper should leave little doubt, however, that the discrete nature of the redshift is not dependent in its demonstration on redshift-magnitude bands. The bands presumably are a still higher order manifestation of a fundamental process which operates on matter through galactic nuclei. In examining subtleties such as the population modulation of adjacent discrete redshift states it is apparently necessary to restrict analysis to within one band. Population phase shifts or modulation frequency shifts might occur anywhere but band boundaries are obvious candidates. When the power spectrum analysis in the 6500 -8000 km s^{-1} interval is extended to the higher and lower redshift data, there is a pronounced drop in the power of the 222 km s^{-1} periodicity. It follows, therefore, that a regular 3-state periodicity is not a general property of the entire redshift distribution. The only periodicity which appears to be independent of bands is the basic 70-75 km s^{-1} effect. We shall therefore now examine the data for that periodicity.

To detect a periodicity in a mass of data of mixed quality the data must be segregated according to quality. The effect sought must then be found consistently in the best data and progressively be lost in the noise as poorer data are considered. Thus the approach used here will be not only to show the presence of a periodicity but also that its detection from sample to sample varies in the way expected as the data

quality varies. Although power spectral methods could be used a more visible direct χ^2 analysis will be employed here. If a distribution has a periodicity P, then successive maxima and minima will be spaced by P/2. We shall proceed by dividing the half period interval into four cells of equal width and examine the cell population against the hypothesis that the cells are equally populated.

The accuracy of the Coma redshift data in Table 2, especially for the emission line and multiple spectra galaxies, is apparently sufficient to show the basic periodicity fairly clearly. The two strongest clumps of points in Figure 9, near 7220 and 7450 km s^{-1}, suggest a distinctly double structure. Since the periodicity expected is known fairly closely, the denser part of the Coma redshift distribution is easily shown to fit a periodicity near 72.5 km s^{-1}. The entire Coma sample extends over about sixty cycles, hence when the more extreme data is considered the periodicity can be found to about 0.1 km s^{-1}. Making one final assumption, discussed in the following section, that the periodicity has a peak point at zero redshift, we find that the relationship

$$Vo = 72.464n \qquad (5)$$

will satisfy the data. The final figure is for bookkeeping only. We now consider the significance of this periodicity in the data.

Using equation 5, the Vo value closest to each observed redshift was calculated and a residual, Δ, formed. The number of residuals in each of the four cells $|\Delta| \leq 9$, $10 \leq |\Delta| \leq 18$, $19 \leq |\Delta| \leq 27$, and $|\Delta| \geq 28$ were tabulated for various data samples. The results are contained in Table 3. Each sample is identified and in addition to the cell populations a "contrast" $|\Delta| \leq 18/|\Delta| \geq 19$ of the periodic distribution is given. The two highest precision samples, emission line and multiple spectra galaxies, give the greatest contrast while the less reliable galaxies selected by H-K residual give a lower contrast

as statistically expected. The χ^2 test for the uniform distribution hypothesis is rejected at nearly the 10^{-3} level.

The lowest part of Table 3 contains the redshift distribution for all the remaining Coma region galaxies not qualifying for one of the more accurate Coma classes or one of the accurate foreground classes to be discussed in the next section. The data are derived from the total sample given by Tifft and Gregory (1976) updated with a few additional new redshifts. The sample is separated according to magnitude. The brighter part, presumably statistically slightly more accurate, shows a very slight contrast in the periodic sense while the fainter part shows none. The χ^2 test shows the sample to be flat as it must be with the uncertainty associated with the redshifts in this sample.

The number of points involved in the 72.46 km s^{-1} periodicity analysis is large. Fully 1/4 of the total sample fall in the more accurate classes. Much can and will be done to further improve the accuracy of redshift data, however, the chance of reversing the trend of a periodic behavior in the redshift distribution of normal galaxies, at least within clusters, is rather small. In the framework of normal dynamics such a periodicity should not exist.

As a final point with regard to clusters we return to the basic Virial mass discrepancy. Rood (1974 with earlier references) shows that the mass discrepancy varies, within uncertainty, directly as σ_v^2. The Virial mass of a cluster depends directly upon σ_v^2 whereas the visible mass depends upon counted numbers of galaxies. Within the sample of rich clusters considered by Rood, there is relatively little variation in visible mass compared to the range in σ_v^2. The dependence of "mass excess" on σ_v^2 can be readily explained if redshift has nothing to do with mass in a dynamical sense. The same is true of any lack of correlation of σ_v^2 and cluster radius, the other dynamical parameter. The point to be made, therefore, is that not

only is the discrete redshift-non-interactive galaxy hypothesis an explanation of the Virial discrepancy, but it predicts the observed functional form of the discrepancy. Up to the limit of the available data, the concept of discrete redshifts and non-interaction of galaxies is viable and consistent.

INTERCLUSTER MOTION

For all of the galaxy subsystems so far considered, individual galaxies, pairs, and clusters, it has been possible to demonstrate that the only real motion consistent with existing observations is rotation and expansion of individual galaxies. Is it possible to go further and determine if individual clusters are at rest or in motion with respect to one another? In order to demonstrate that no appreciable motion exists on a large scale one must show that the redshift periodicity in independent objects or clusters phases together perfectly. Some evidence that such phasing occurs has been given by Tifft (1973, 1974), however, limitations in redshift precision and galactic rotation corrections make this test very difficult.

One approach to the question is to utilize nearby groups of galaxies and study their relationship to the Local Group. At the present time the M101 group appears to be one of the best candidates to introduce such an analysis. Sandage and Tammann (1974) have examined the M101 group and demonstrated that the group participates in the smooth redshift-distance relationship required by either the expanding universe cosmologies or the static time dependent redshift cosmology implied in this paper. Figure 10 is a plot of predicted redshifts extrapolated outward from the Local Group

with a periodicity near 72.5 km sec^{-1}. The five minor galaxies in the M101 group are plotted, with uncertainties, at their 21 cm redshifts as listed by Sandage and Tammann (1974). M101 is shown with a dashed vertical line. All the galaxies except M101 are consistent with the predicted redshifts. The situation regarding M101 itself is interesting. Figure 11 is a plot of 21 cm redshifts along the major axis adapted from Rogstad (1971). It is quite apparent that the central redshift of M101 is derived from symmetry assumptions in the rotation curve and is not the actual central redshift. The diagram is readily interpreted, as shown, in terms of the dual redshift stream concept blurred by limited radio resolution. The galaxy can be represented with two redshifts, a dominant one about 30 km sec^{-1} higher and a lesser one about 40 km sec^{-1} lower than the central value assumed by Rogstad. The "peculiar" ridge of intensity on the dominant side of the galaxy is now readily explained. Figure 10 displays the two suggested redshifts for M101 as open circles, the larger one for the dominant higher redshift. With this interpretation, fully consistent with the observation, M101 is now in agreement with the general periodic redshift pattern.

As a second demonstration of the universal nature of the basic redshift periodicity, extrapolated outward from a local value of zero, we will reconsider the investigation of the Coma cluster region given in the previous section. The step from the local galaxies to the Coma clsuter represents nearly 100 cycles of the 72.5 km sec^{-1} periodicity. For a jump of this many cycles phasing or correlation can easily be lost and the forcing of the Coma periodicity to pass through zero locally could be artificial. Two arguements against this may be given, however. The first concerns the range of redshift within the Coma cluster, and the second foreground galaxies in the Coma field. Data on foreground

galaxies are contained in Table 4.

Not shown in the previous section was the fact that, unlike the 3-cycle 222 km sec^{-1} periodicity, the final Coma 72.46 km sec^{-1} periodicity fits equally well over the full 60 cycle range of redshift present in the Coma cluster. This is shown in Table 5 for five redshift intervals. Within the accuracy of the data there is no drift in contrast or cell population as one goes away from the central redshift in the Coma cluster. If as much as one cycle were gained or lost in the cycle count between here and Coma there would be a drift of more than ½ cycle from one extreme of the Coma distribution to the other. Thus the Coma periodicity, determined internally within the cluster is consistent with being strictly in phase with the local periodicity determined from the Local Group and M101 group.

If we have a periodicity in phase locally and at the Coma cluster distance then the next logical test of the absolute nature of the periodicity is to identify objects at intermediate distances and examine their periodicity and phasing. Two groups are available to investigate this question, the Coma I group and a group near 2500 km sec^{-1} identified by Tifft and Gregory (1976). For the 2500 km sec^{-1} group we use emission line redshifts from Tifft and Gregory (1976) of the caliber of the best Coma emission line values. For Coma I we use data summarized by Chincarini and Rood (1976, called CRN in the table) supplemented by a few galaxies in the list of Tifft and Gregory (1976, called X or specific source given in the table). Except for one galaxy with a redshift by the author these galaxies have redshifts from mixed sources. Emission is, however, common in these galaxies and they are relatively bright, thus there is reason to believe the redshift data are relatively accurate.

The middle part of Table 3 shows that the 72.46 km s^{-1} periodicity anchored at zero and Coma redshifts is present and in phase with the foreground groups. The periodicity test in the foreground groups is not in itself quite significant, however, the point here is the phasing assuming the periodicity. When the small foreground sample is added to the best Coma sample, they clearly reinforce and reject the uniform distribution hypothesis at the 3×10^{-4} level. Even the complete 332 galaxy sample, degraded as it is by the low quality redshifts, shows the periodicity at the 98 percent level of significance. At no scale in the Universe beyond the scale of single rotating and expanding galaxies would significant motion seem to be required.

It has been suggested by Vorontsov-Velyaminov (1969) that clusters of galaxies arise as fragmentation products of parent objects such as QSS. This viewpoint is consistent with the concepts developed in this paper excepting that violent ejection is not required or permitted. The very slow motions required, spread over a long history of fissioning, could perhaps produce what we call clusters today. It is interesting, from the viewpoint of fissioning, that the magnitude spacing of the redshift-magnitude bands in Coma and A2199 is close to what would be produced by a hierarchy of fissioning of standard parent bodies into equal parts. The sloping of the bands toward fainter magnitude with increasing redshift requires that the parent bodies have other special properties such as luminosity evolution in time. Galactic nuclei would appear to be highly constrained in their properties.

IMPLICATIONS

The thrust of this paper and its predecessor has been to present empirical evidence for three main concepts, the existence of the discrete

redshift, the distribution of redshift states into a two stream model in individual galaxies, and the non-interaction of galaxies on a large scale. Assuming that the concepts are at least partially correct, and the evidence is not negligible at this stage, it is of interest to point out one possible implication. There is little doubt that material within any given redshift state experiences self gravitation. Individual stars, gas clouds, etc. obviously form within each redshift stream in galaxies. It is not at all obvious, however, that a normal attractive gravitational force applies between the streams or states. They have odd boundary interactions and do not appear to readily mix. The boundary situation and the net expansion of galaxies in opposed streams suggest that the streams could repel. If this is the case, the internal dynamics of a galaxy will depend upon the local combination of normal gravitation and what I shall define as a possible interstate force or ISF. If a galaxy is viewed at a sufficient distance, the net force felt will be the resultant of gravitation and ISF. If the two are equal and opposite, we can have, in effect, a dipole and no net force between galaxies. Other concepts may well be preferable in explaining non-interaction, but it is not clear that they can explain the internal pattern in individual galaxies. Discrete states of redshift appears to imply fundamentally different states of matter, at least a quantized electron mass. Our understanding of gravitation is certainly limited and it may not be completely unrealistic to suggest that different states of matter could have different gravitational properties.

One final point that is apparently easily misunderstood can perhaps be clarified here. In a static and non-interactive Universe, the variation of redshift with distance (Hubble law) requires an evolutionary effect in matter with time (distance). However, the inverse Hubble constant does not give a

time since origin as in dynamical cosmologies. The origin time is not obviously related to H at all. Galaxies can exist long before they become "visible" at any redshift so there is no limit to the time available for galaxies to separate at very slow speeds.

ACKNOWLEDGEMENT

The author gratefully acknowledges discussions with Drs. J. Cocke, J. Scott, A. Pacholczyck, and Mr. T. Sargent relating to the distribution of projection factors in double galaxies.

TABLE 1

Differential Redshifts in the Doubled Lines of Galaxy Pairs

N	K83	K144	K181	K252	K288	K363	K466
0			15				
1				65			
2							
3					207		
4	294	297		277			288
5						365	

TABLE 2

Best Redshifts Within 6^{o} of Coma

Identification		Vo	Source	m_p	R
		6500-8000 Multiple Spectra			
160A-03	I3949	7419	C3	14.9	0.25
07	I3955	7687	C3	15.6	0.16
09	I3959	7006	C3	15.2	0.25
12	N4864	6769	C4	14.8	0.14
16	N4869	6801	C3	14.9	0.11
17	I3976	6777	C3	15.1	0.14
18	N4871	6757	C3	15.1	0.07
21	N4872	7258	C3	15.3	0.06
22	N4874	7180	C3	13.7	0.06
23	N4875	7866	C3	15.6	0.07
25	N4976	6739	C3	15.1	0.06
29	N4881	6725	C3	14.7	0.28
32	N4889	6521	C5	13.0	0.06
35	I4012	7248	C3	15.7	0.13
39W	N4898W	6812	C3	(15.2)	0.10
44	N4906	7510	C3	15.2	0.20
47	I4045	6865	C3	15.1	0.24
160-065	RB241	7185	C3	15.0	0.30
		6500-8000 Emission Lines			
130-008		7387E	K	14.9	2.89
159-037	N4585	7411E	E1αβ	14.6	4.86
049	I3645	6532E	CT	15.4	4.54
059		7456E	CT	14.5	3.72
101		7846E	CR+GN	15.3	1.68
102		7012E	E1β	14.5	1.60
160A-43	I4040	7613E	E2β	15.1	0.17
160-055	N4848	7272E	E1β	14.2	0.47
058		7674E	E1α	15.5	0.83
064		7423E	E1αβ	15.4	0.78
067		7689E	CR+K	15.4	0.85
086		7481E	C1αβ	15.4	0.35
096N	N4922N	7029E	H1β	(15.5)	1.39
188-024		7170E	E1αβ	14.2	5.59
	C6.124	7478E	E1αβ	(16.0)	0.8
		6500-8000 K-H < 50			
160A-11	I3963	6645	C1	15.7	0.23
51	N4911	7831	C1	13.7	0.29
160-028	N4827	7498	E1	14.1	1.06
046S	N4842S	7496	E1	14.9	0.69
094	N4919	7278	C1	14.9	0.37
099	I 843	7416	E1	14.8	1.23

Identification		Vo	Source	m_p	R
160-107		7246	E1	14.9	1.37
147	N4983	6520	C1	14.9	1.92
158		7034	E1	14.6	4.37
166	N5032	6536E	E1A	13.6	3.00
168	N5041	7471	E1	14.2	4.21
	4000-6500, 8000-10000 Multiple Spectra				
160A-01	I3946	6009	C3	15.3	0.28
26	RB 49	8037	C3	15.6	0.10
28	N4883	8051	C3	15.2	0.06
41	I4026	8198	C3	15.5	0.15
160-070	N4854	8276	C3	15.2	0.37
	RB113	8471	C3	(16.0)	0.19
	RB119	8608	C4	(16.0)	0.22
	4000-6500, 8000-10000 Emission Lines				
159-034		6432E	CT	15.7	5.10
035		4591E	CT	15.5	5.01
051S		9489E	CT	15.4	4.19
054		4477E	CT	15.5	4.32
082		8174E	E1α	14.8	3.65
097		6477E	E1αβ	15.4	1.97
160A-04	N4858	9500E	E1β	15.5	0.24
160-020N		4982E	E1αβ	15.5	0.87
073	RB219	5354E	C1β	15.1	0.36
076		5342E	CR	15.6	0.67
108		8323E	CR	15.5	0.58
127		5627E	G	15.5	1.21
128		8066E	CR	15.3	1.31
139		4854E	G	15.0	1.72
151		6462E	CR+K	15.1	2.50
181		5732E	E1αβ	14.3	4.94
183		5720E	E1αβN	14.7	5.34
202		5183E	E1α	14.9	5.69
	TT 5	8180E	E2αβ	(16.0)	0.4
	TT 15	8970E	E1β	(16.0)	0.6
	4000-6500, 8000-10000 K-H < 50				
159-092	N4738	4791	E1	14.9	2.09
113	N4789	8224	E1	13.3	1.52
160A-02	I3947	5700	C1	15.6	0.28
05		8028	C1	15.3	0.31
50	I4051	4926	C2	14.8	0.24
160-044E	N4841E	6224	E1	14.3	0.73
162		6394	E1	14.6	4.75

TABLE 3

Distribution of Coma Galaxies

for Periodicity 72.464n

Class	$\Delta \leq 9$	$10 \leq \Delta \leq 18$	$19 \leq \Delta \leq 27$	$28 \leq \Delta$	$\Delta \leq 18 / \Delta \geq 19$
		Coma Best Galaxies			
Emission	14	11	7	3	2.5
3 Spectra	10	8	3	4	2.6
K-H≤50	8	3	3	4	1.6
Total Best Coma	32	22	13	11	χ^2=14.2 p=0.003 n=78
		Best Foreground			
Coma I	15	6	9	5	} 1.9
2500 Group, Emission	1	4	0	0	
Total Best Foreground	16	10	9	5	χ^2=6.2 p=0.1 n=40
Total Best Sample	48	31	22	17	χ^2=18.9 p=0.0003 n=118
		Remaining Low Precision Galaxies			
m_p<15.0	21	20	14	19	1.2
$m_p \geq 15.0$	34	38	33	35	1.0
Total Low Precision	55	58	47	54	χ^2=1.2 p=0.75 n=214
Entire Sample	103	89	69	71	χ^2=9.3 p=0.025 n=332

TABLE 4

Best Redshifts in the Coma Foreground

Identification		Vo	Source	m_p
		Coma I, Chincarini and Rood		
129-005	N4494	1305	CRN	10.7
027	N4725	1213	CRN, X	10.2
028	N4747	1216	CRN, X	13.2
157-072	N4020	800	CRN	13.2
158-008	N4062	744	CRN	11.9
158-012	N4080	722	CRN	14.0
014		434	CRN	12.1
037	N4150	236	CRN	12.6
043	N4173	1093	CRN	13.7
059	N4245	882	CRN	12.4
060	N4251	1000	CRN	11.5
071	N4274	761	CRN	11.1
077	N4278	622	CRN	11.2
080	N4283	1078	CRN	13.1
082		1009	CRN	15.0
088	N4308	602	CRN	14.3
092	N4310/11	895	CRN	13.5
093	N4314	879	CRN	11.5
099	N4359	1174	CRN	13.9
104	N4393	829	CRN	13.8
108	N4414	720	CRN	10.9
113	N4448	687	CRN	11.9
159-016	N4525	1136	CRN	13.0
024	N4559	852	CRN, X	10.7
065	N4656/7	775	CRN, X	10.6
069	N4670	1112	CRN, X	12.6
074		862	CRN, X	15.0
187-029	N4203	1008	CRN	11.8
042	N4395	324	CRN	11.7
188-015	N4627	745	CRN	13.3
016	N4631	646	CRN, X	9.8
		Coma I, Tifft and Gregory		
129-008	N4562	1379E	E1βγ, CRN	14.6
010	N4565	1171E	RC	10.3
159-067		943E	CT	14.7
160-160		877E	K	14.6
		2500 Group with Strong Emission		
130-019	N5016	2769E	E1β	14.3
020		2592E	E1β	14.8
160-134	N4961	2591E	E1β	13.5
194	N5089	2190E	E1αβ	14.4
161-037	N5117	2465E	E1β	14.5

TABLE 5

Redshift Periodicity as a Function of Redshift in the Coma Cluster

Redshift Range	Cell Population	Contrast
4500-5500	4/2/2/1	6/3
5500-6500	4/3/2/1	7/3
6500-7500	13/10/6/7	26/13
7500-8500	9/5/3/2	14/5
8500-9500	2/2/0/0	4/0

REFERENCES

Casini, C. and Heidmann, J. 1975, Astron. and Astrophys. 39, 127.

Casini, C., Heidmann, J., and Lolievre, G. 1974, IAU European Assembly Section C, Trieste.

Chincarini, G. and Rood, H. 1976, Ap.J., in press.

deVaucouleurs, G. and deVaucouleurs, A. 1964, Reference Catalogue of Bright Galaxies, University of Texas, Austin.

deVaucouleurs, G. and deVaucouleurs, A. 1967, A.J. 72, 730.

Gorbachëv, B. I. 1971, Soviet A.J. 14, 939.

Heidmann, J. and Kalloghlian, A. T. 1973, Astrofizica 9, 71.

Heidmann, J. and Kalloghlian, A. T. 1975, Astrofizica, in press.

Jenner, D. C. 1974, Ap.J. 191, 55.

Karachentsev, I. D. 1972, Comm. Special Astrophysical Obs. USSR 7, 1.

Karachentsev, I. D. 1974, Comm. Special Astrophysical Obs. USSR 11, 51.

Karachentsev, I. D. and Shcherbanovsky, A. 1970, Acta Astron. 20, 373.

Noerdlinger, P. D. 1975, Ap.J. 197, 545.

Page, T. L. 1952, Ap.J. 116, 63.

Rogstad, D. H. 1971, Astron, and Astrophys. 13, 108.

Rood, H. J. 1974, Ap.J. 194, 27.

Sandage, A. and Tamman, G. A. 1974, Ap.J. 194, 223.

Tifft, W. G. 1973, Ap.J. 181, 305.

Tifft, W. G. 1974, The Formation and Dynamics of Galaxies, IAU Symp. 58, ed. J. R. Shakeshaft, Reidel Publ. p. 243.

Tifft, W. G. 1976, Ap.J. in press (June).

Tifft, W. G. and Gregory, S. A. 1976, Ap.J. in press (April).

Tifft, W. G. and Tarenghi, M. 1975, Ap.J. 199, 10.

Toomre, A. and Toomre, J. 1972, Ap.J. 178, 623.

Vorontsov-Velyaminov, B. 1969, A.S.P. Leaflet No. 485.

Zonn, W. 1968, Acta Astron. 18, 549.

Zwicky, F. and Herzog, E. 1963, Catalogue of Galaxies and Clusters of Galaxies, Vol. 2, Calif. Inst. of Tech., Pasadena.

FIGURE CAPTIONS

Figure 1 The distribution of the observable fraction of the true relative velocity and separation for randomly oriented pairs of galaxies.

Figure 2 Differential redshifts in double galaxies as a function of total absolute magnitude of the pair. Data are from Karachentsev (1974). Pairs are separated into morphological groups. Filled circles refer to pairs with projected separations less than 40 kpc while crosses denote wider pairs. Note especially the large number of luminous low ΔV spiral-spiral pairs.

Figure 3 The frequency distribution of differential redshifts in double galaxies up to 400 km sec^{-1} and combined $Mp<-19$ according to Karachentsev (1974). The upper panel includes spiral-spiral pairs while the middle panel is for pairs containing one or two ellipticals. The lower panel is for pairs showing no sign of physical interaction.

Figure 4 The distribution of projected separations and the relationship of separation and differential redshift for double galaxies up to 40 kpc projected separation according to Karachentsev (1974). Spiral-spiral pairs are shown on the left side. Open circles refer to pairs with combined magnitude brighter than $-21.0=Mp$ while filled circles refer to pairs with combined magnitude $-21<Mp<-19$. Pairs with

(Fig. 4) one (crosses, dashed line) or two (filled circles, solid line) ellipticals are shown on the right.

Figure 5 M/L ratios derived for double galaxies by Karachentsev (1974) as a function of combined absolute magnitude in spiral-spiral pairs. The solid line is a line of constant mass.

Figure 6 The redshift differences between double galaxies as tabulated by Karachentsev (1974). The upper (a) panel gives the distribution for all pairs with differences less than 600 km sec^{-1}, while the lower (b) panel includes only those pairs with uncertainties estimated to be less than 100 km sec^{-1}. In both cases the distribution peaks at aero and has suggestions of preferred discrete values.

Figure 7 The power spectrum of the distribution of redshift differences in double galaxies using the 56 most accuarate examples shown in Figure 6b.

Figure 8 The distribution of redshift in the Local Group of galaxies. The distribution appears periodic at close to the expected redshift state spacing. Most galaxies bunch at one preferred redshift rather than distributing uniformly over several adjacent states. Filled circles refer to the spirals, open circles to irregulars, crosses to dwarf ellipticals and the plus sign to a dwarf spheroidal.

Figure 9 The upper (a) panel gives the redshift-m_p diagram for the most accurate redshift determinations in the Coma cluster in the redshift interval 6500-8000 km sec^{-1} and less than

(Fig. 9) 6^{o} from the cluster center. Filled circles are multiple spectrum means for absorption line galaxies, open circles are relatively strong emission line galaxies, and crosses refer to high quality spectrograms with the best internal H and K agreements. The middle (b) panel shows the redshift distribution of the sample, and the lower (c) panel gives the power spectrum. There is clear evidence for a discrete structure at a spacing of three times the standard state spacing.

Figure 10 The relationship of redshift in the Local Group and the M101 group. Predicted redshifts for galaxies extrapolated from the Local Group are shown shaded. The five small galaxies in the M101 group are shown at their 21 cm redshifts with error bars. M101 is shown with a vertical dashed line and is decomposed into two redshifts as discussed in the text and Figure 11.

Figure 11 The major axis 21 cm rotation curve of M101 adapted from Rogstad (1971). An interpretation of the rotation curve with a dual redshift pattern is shown with the dotted lines. The suggested pattern matches the HI ridge which does not fit the usual symmetrical single valued curve.

PLATE CAPTIONS

Plate 1 Enlargements of sections of 47Amm^{-1} spectrograms of eight Karachentsev (1972) double galaxies obtained with the 90-inch Steward Observatory telescope at Kitt Peak. Both spatial and redshift doubling of emission lines is common. The redshift doubling always appears to occur in multiples of the basic redshift state spacing.

MAILING ADDRESS

W. G. Tifft
Steward Observatory
University of Arizona
Tucson, Arizona 85721

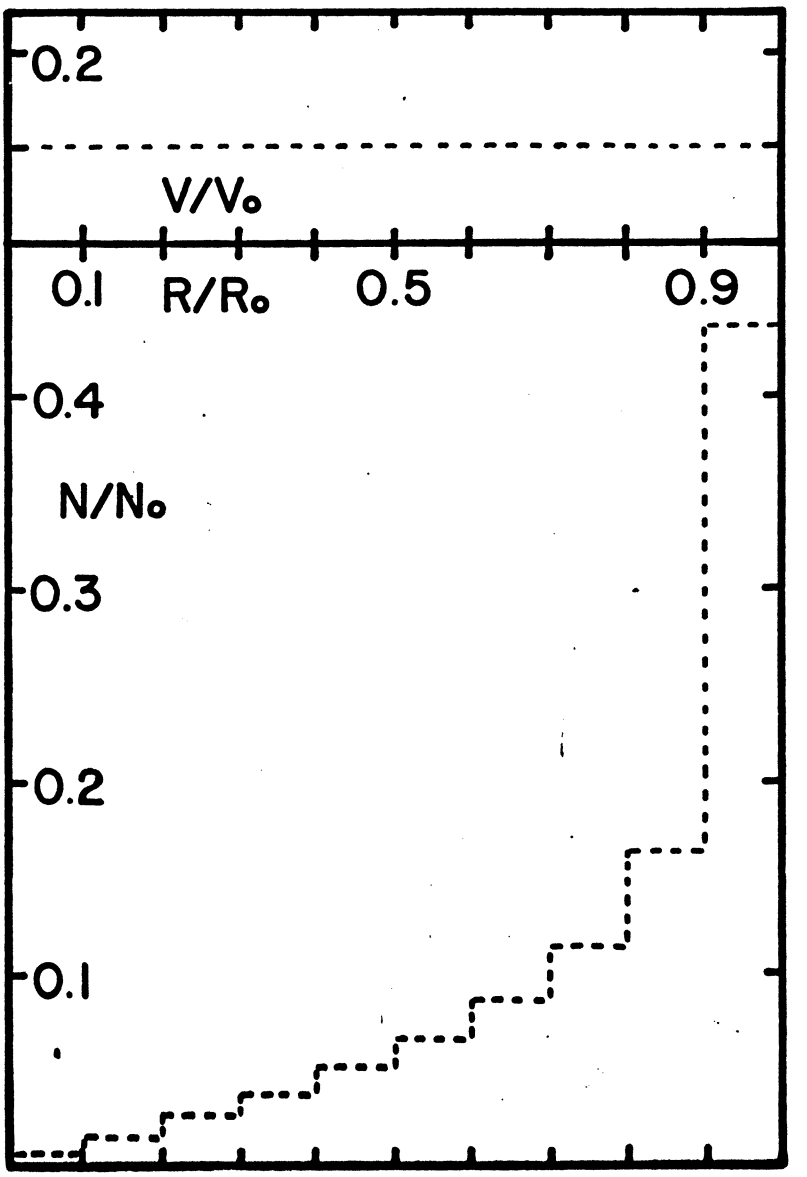
0.2
V/V₀
0.1
R/R₀
0.5
0.9
0.4
N/N₀
0.3
0.2
0.1

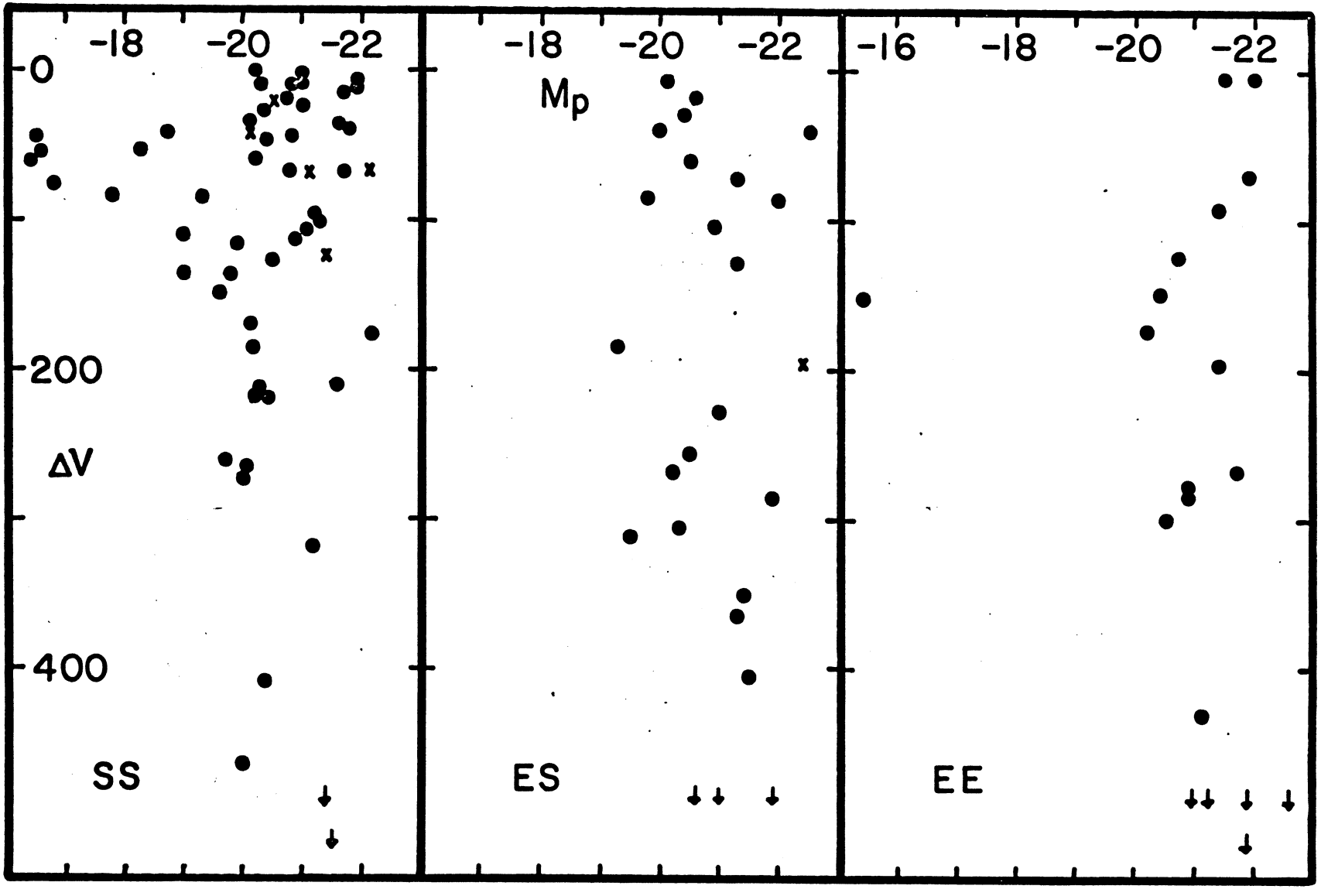
-18
-20
-22
0
200
400
ΔV
SS
-18
-20
-22
Mp
ES
-16
-18
-20
-22
EE

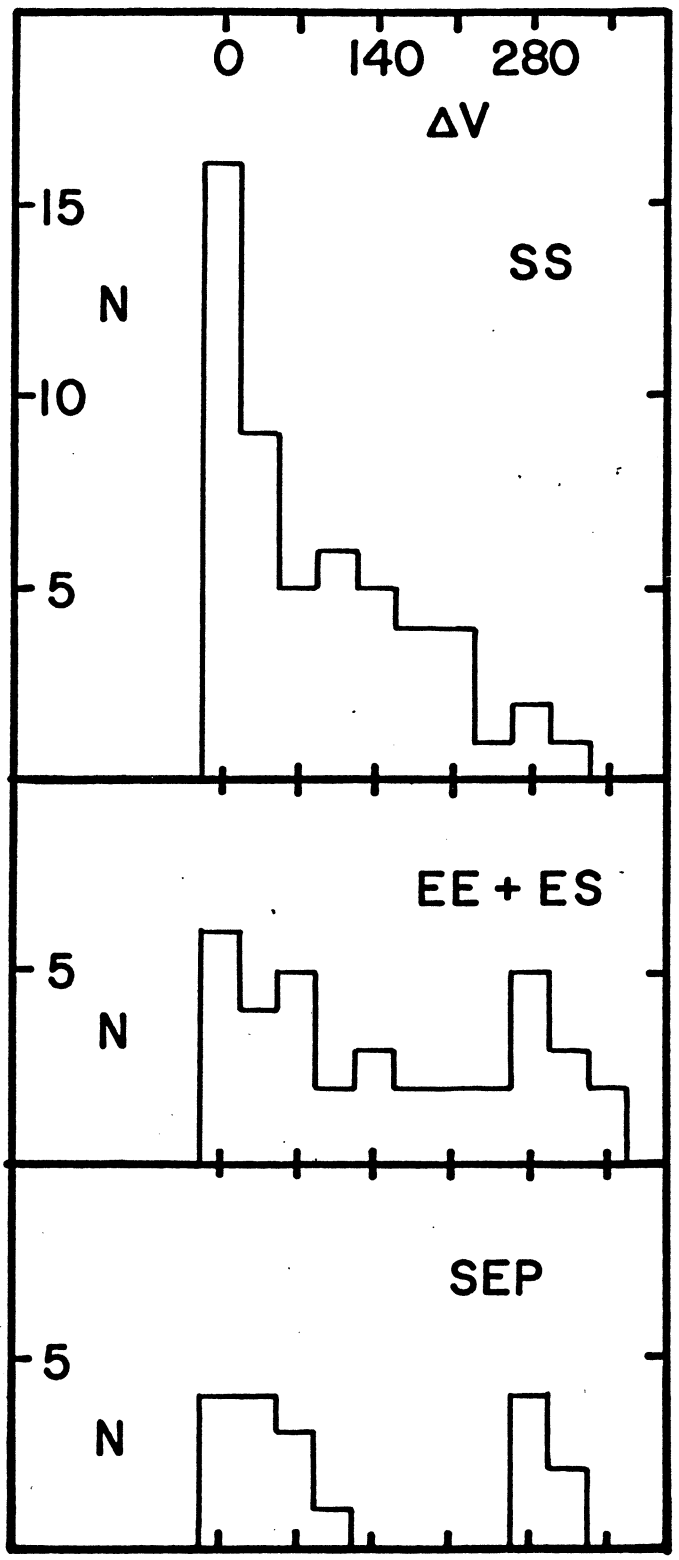
0
140
280
ΔV
15
N
10
5
SS
EE + ES
5
N
SEP
5
N

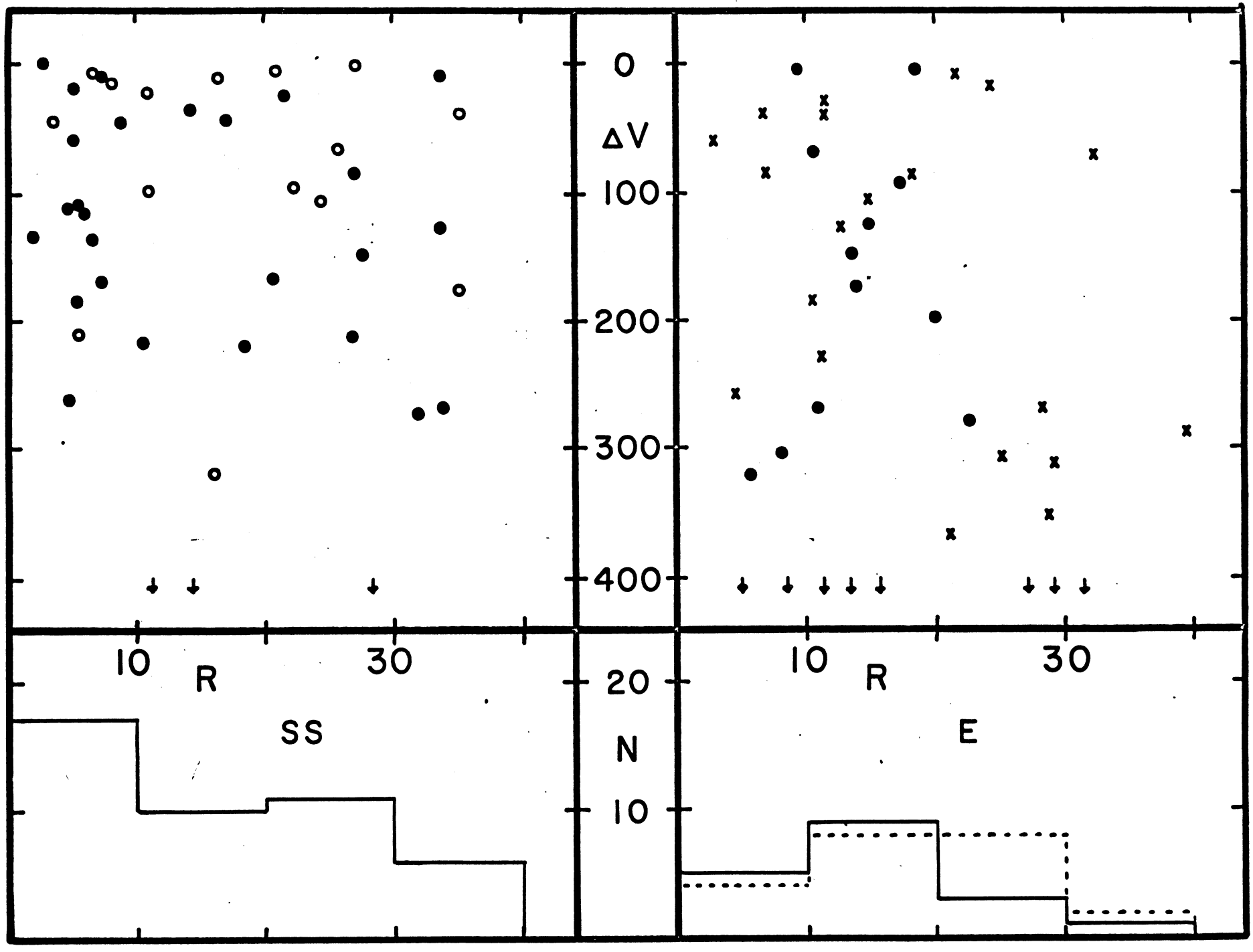
0
ΔV
100
200
300
400
10
R
30
SS
20
N
10
10
R
30
E

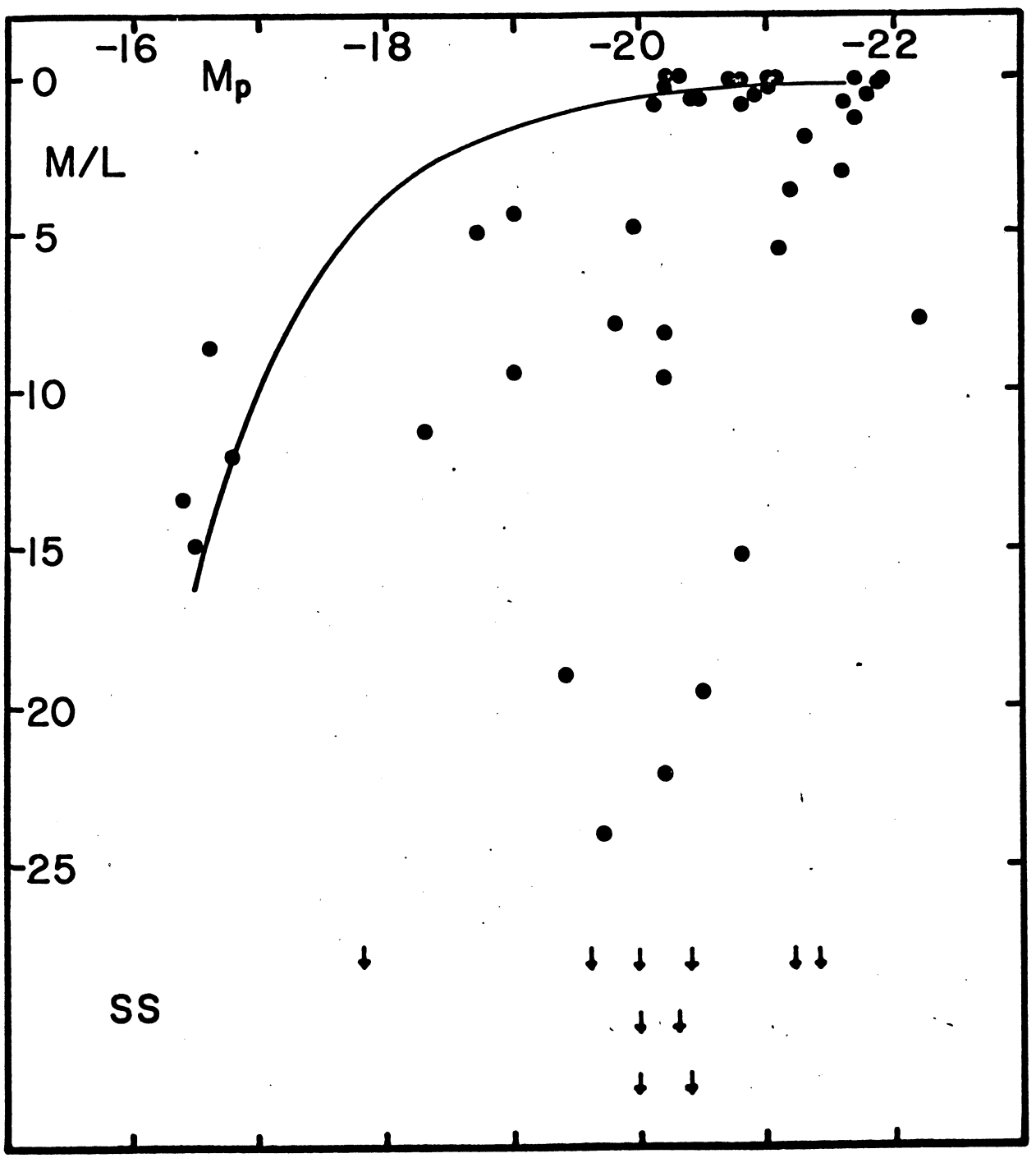
-16
-18
-20
-22
0
M_p
M/L
5
10
15
20
25
SS

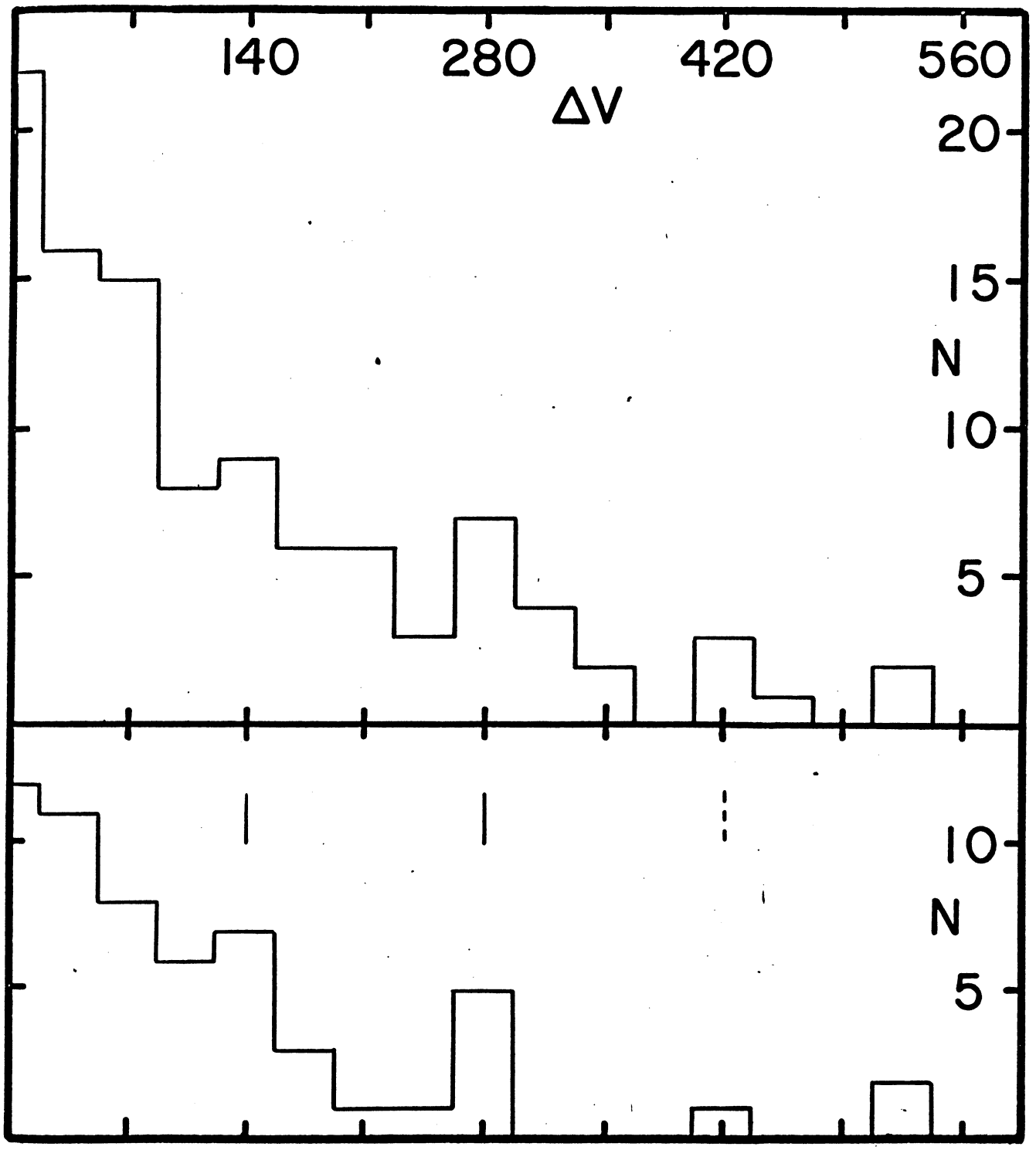
140
280
420
560
ΔV
20
15
N
10
5
10
N
5

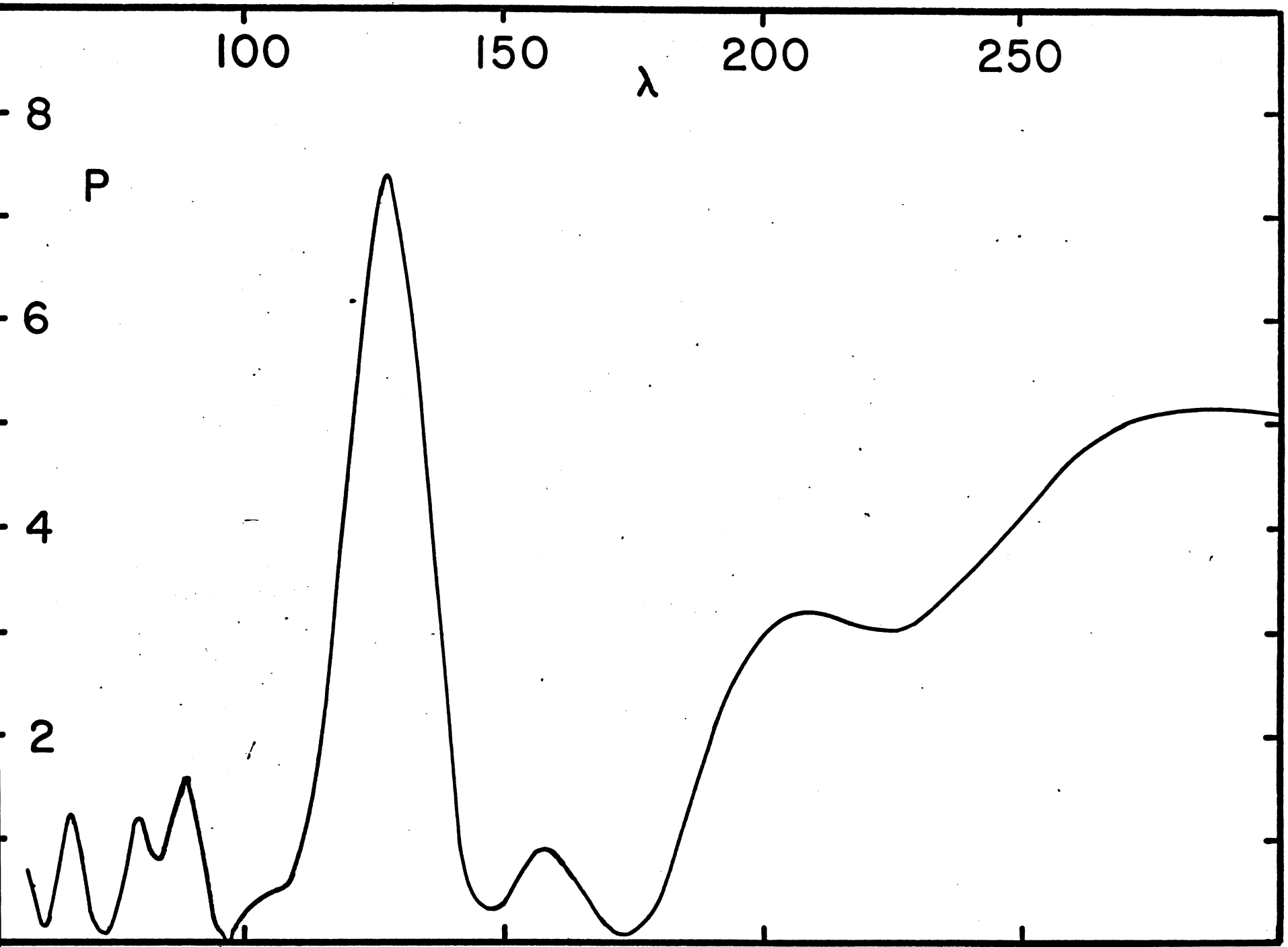
100
150
λ
200
250
8
P
6
4
2

T.S.E. (3)

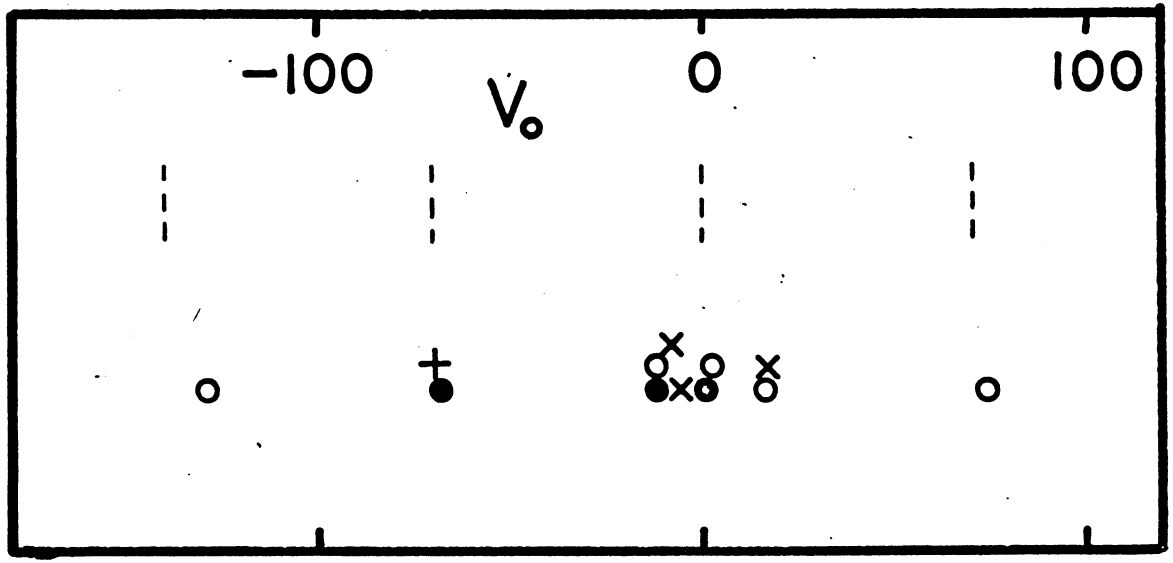

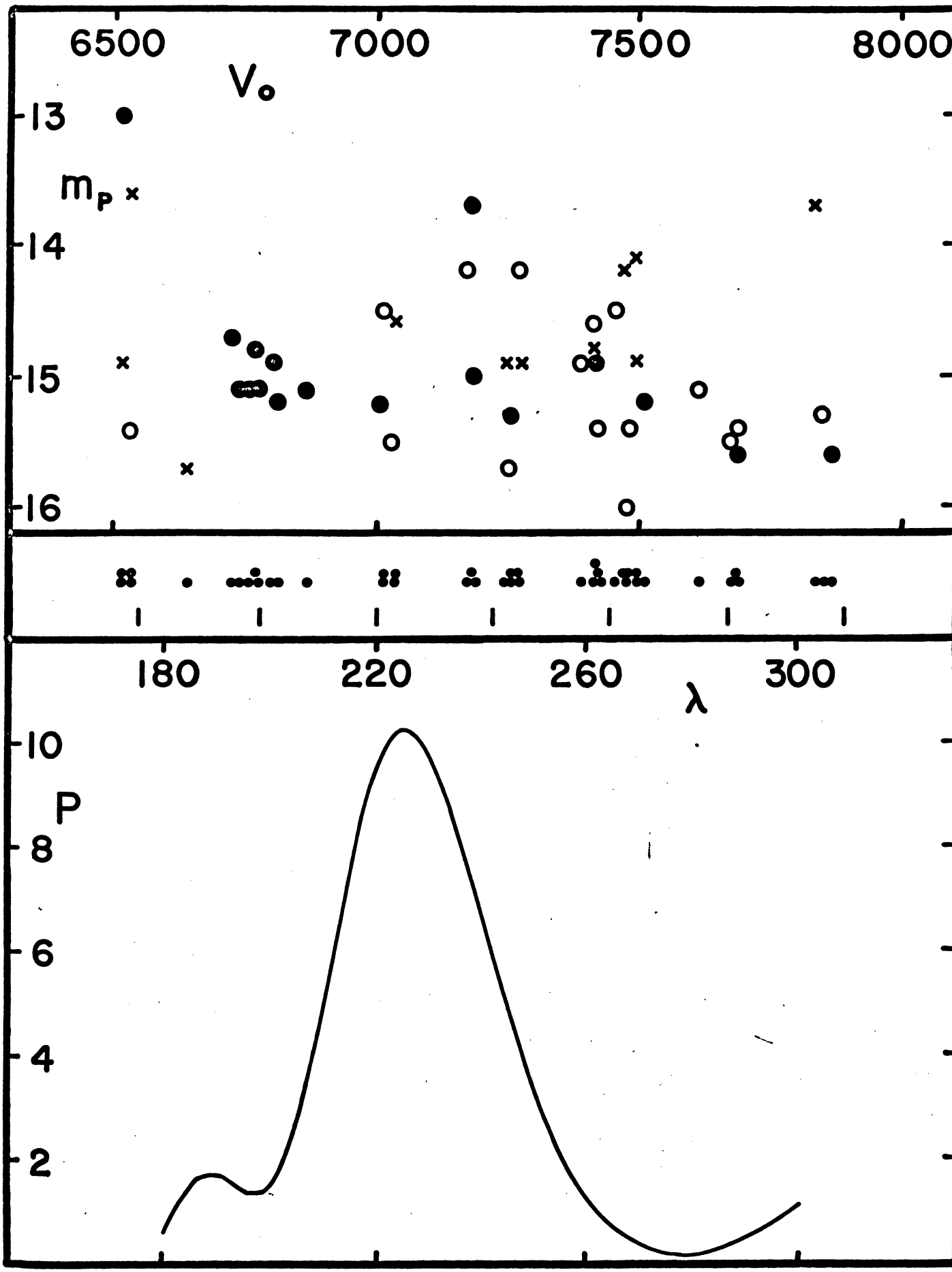
6500
7000
7500
8000
V_o
13
m_p
14
15
16
180
220
260
300
λ
10
P
8
6
4
2

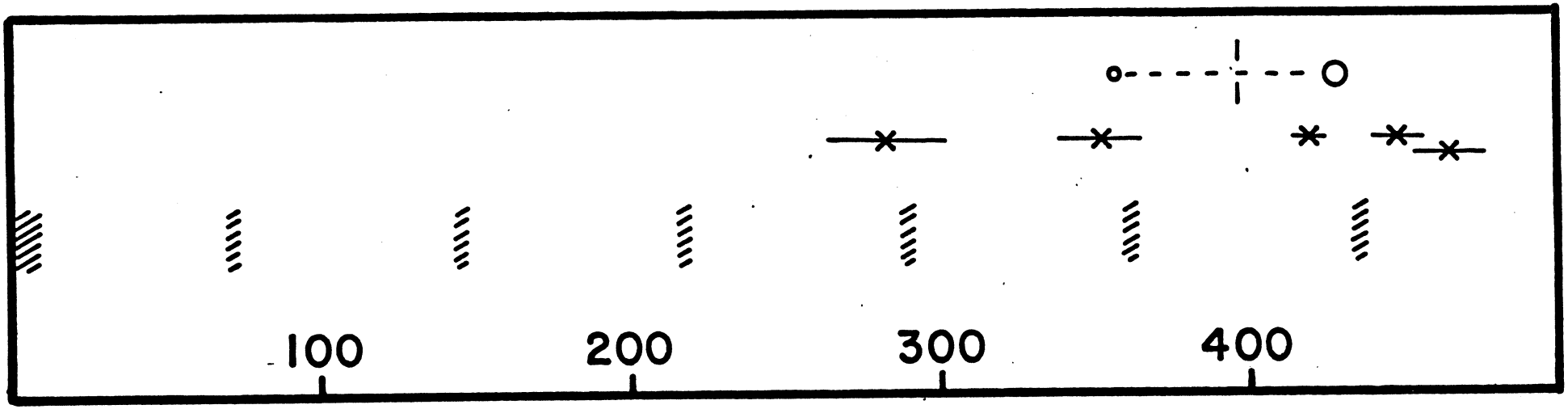
100
200
300
400

Tilt (11)